the FEBS Journal

Altered expression of CD1d molecules and lipid accumulation in the human hepatoma cell line HepG2 after iron loading

Marisa Cabrita[1,*], Carlos F. Pereira[1,*], Pedro Rodrigues[1,3], Elsa M. Cardoso[2] and Fernando A. Arosa[1,3]

1 Institute for Molecular and Cell Biology (IBMC), Porto, Portugal
2 Instituto Superior de Ciências da Saúde – Norte (CESPU), Gandra, Portugal
3 Instituto de Ciências Biomédicas Abel Salazar (ICBAS), Porto, Portugal

Keywords
liver, iron, CD1d, MHC, lipids

Correspondence
F. A. Arosa, Institute for Molecular and Cell Biology, Rua do Campo Alegre, 823, 4150–180 Porto, Portugal
Fax: +351 226092404
Tel: +351 226074900
E-mail: farosa@ibmc.up.pt

*These authors contributed equally to the paper

(Received 8 July 2004, revised 13 September 2004, accepted 18 September 2004)

doi:10.1111/j.1432-1033.2004.04387.x

Iron overload in the liver may occur in clinical conditions such as hemochromatosis and nonalcoholic steatohepatitis, and may lead to the deterioration of the normal liver architecture by mechanisms not well understood. Although a relationship between the expression of ICAM-1, and classical major histocompatibility complex (MHC) class I molecules, and iron overload has been reported, no relationship has been identified between iron overload and the expression of unconventional MHC class I molecules. Herein, we report that parameters of iron metabolism were regulated in a coordinated-fashion in a human hepatoma cell line (HepG2 cells) after iron loading, leading to increased cellular oxidative stress and growth retardation. Iron loading of HepG2 cells resulted in increased expression of Nor3.2-reactive CD1d molecules at the plasma membrane. Expression of classical MHC class I and II molecules, ICAM-1 and the epithelial CD8 ligand, gp180 was not significantly affected by iron. Considering that intracellular lipids regulate expression of CD1d at the cell surface, we examined parameters of lipid metabolism in iron-loaded HepG2 cells. Interestingly, increased expression of CD1d molecules by iron-loaded HepG2 cells was associated with increased phosphatidylserine expression in the outer leaflet of the plasma membrane and the presence of many intracellular lipid droplets. These data describe a new relationship between iron loading, lipid accumulation and altered expression of CD1d, an unconventional MHC class I molecule reported to monitor intracellular and plasma membrane lipid metabolism, in the human hepatoma cell line HepG2.

The protein mutated in hereditary hemochromatosis (HFE) is an unconventional MHC class I molecule involved in the regulation of intracellular iron metabolism through poorly understood molecular mechanisms [1,2]. Although *HFE* mutations are clearly associated with iron overload both in humans and mice [1,3,4], the marked clinical heterogeneity among affected individuals with the same mutations indicates that other molecules, environmental factors, and cells of the immunological system probably modify disease severity [5–11]. Recently, it has been demonstrated that in addition to their role as peptide presenting structures, classical MHC class I molecules are involved in the regulation of liver iron metabolism [12].

Abbreviations
DCFH-DA, 2′,7′-dichlorodihydrofluorescein-diacetate; APAAP, alkaline phosphatase-antialkaline phosphatase; MHC, major histocompatibility complex; MFI, mean fluorescence intensity; ROS, reactive oxygen species.

The study of the influence that environmental and genetic factors have on liver iron metabolism, has received great attention over the past years using knockout and transfection technologies. In marked contrast, studies addressing the effect that iron loading of hepatic cells has on the expression of immune recognition molecules have been scarce. *In vivo* studies by Hultcrantz and collaborators showed that iron accumulation in the liver of hemochromatosis patients is associated with oxidative stress and increased expression of ICAM-1 [13]. On the other hand, a recent *in vitro* study examining the effect of iron loading on gene expression in HepG2 cells by differential display revealed that iron can affect mRNA levels of proteins unrelated with iron metabolism, but none was associated with immune recognition molecules [14]. Interestingly, in this study, iron-treated cells showed a marked decrease in Apo B100; a protein essential for maintaining normal lipid metabolism. Hepatic iron overload has been reported in nonalcoholic steatohepatitis [15,16], and an association of hepatic iron stores with steatosis was reported in patients with insulin-resistance syndrome [17]. However, the nature of the relationship between hepatic steatosis and iron overload remains obscure.

CD1d is an unconventional MHC class I molecule specialized in binding and presenting lipids to selected subsets of T cells [2,18,19]. Earlier studies on human CD1d expression showed that this unconventional MHC class I molecule localizes in the cytoplasm of human epithelial cells of the gastrointestinal tract and liver, two central organs in the regulation of iron metabolism [20,21]. After their synthesis in the endoplasmic reticulum, CD1d molecules are continuously recycled between the surface and endolysosomal compartments [22]. Cell surface expression seems to be dictated by the presence of a tyrosine motif in the cytoplasmic tail of CD1d that allows association with several chaperones and adaptors that direct the molecule to endolysosomes, and by its capacity to bind lipid compounds within the different endolysosomal compartments [23].

In this study, we examined whether iron loading of the liver epithelial cell line HepG2 influenced the expression of immune regulatory molecules known to function as ligands of selected subsets of T cells, such as MHC class I and II, CD1d, ICAM-1 and the novel CD8 ligand gp180. We also characterized parameters of oxidative stress, cell growth and lipid metabolism in the iron loaded HepG2. The results of the study revealed a new link between iron loading and lipid accumulation, leading to upregulation of CD1d molecules at the cell surface in HepG2 cells.

Results

Development of iron accumulation in HepG2 cells cultured in iron-rich media

To examine changes in iron metabolism parameters we examined expression of the transferrin receptor, ferritin and storage iron in HepG2 cells grown in media supplemented with 100 μM of ferric citrate (iron-rich media), the most common form of nontransferrin bound iron found in iron overload conditions such as hemochromatosis [24]. The transferrin receptor, CD71, was expressed at moderate levels by HepG2 cells, and culture in iron-rich media decreased its expression (Fig. 1A). Permeabilization with saponin allowed us to determine that HepG2 cells contained high levels of intracellular ferritin, with some ferritin being expressed at the cell surface and culture in iron-rich media increased by two- to threefold the ferritin content as determined by the increase in mean fluorescence intensity (MFI) (Fig. 1C). As shown in Fig. 1B, permeabilization with saponin did not increase background staining when rabbit immunoglobulins were used as first step antibody. The opposite changes in CD71 and intracellular ferritin in HepG2 cells grown in iron-rich media were observed regardless of the time in culture. Under these conditions HepG2 cells showed intracellular iron accumulation as determined by Perls' staining (Fig. 1D). Kinetic experiments showed that iron deposition was detectable after 1 week of culture (≈ 20% of cells positive for iron) and reached a plateau after 8 weeks of culture (≈ 60% of cells positive, Fig. 2A). In all subsequent experiments, HepG2 cells were cultured in iron-rich media for at least 3–4 weeks before any determination unless indicated.

Growth in iron-rich media induces oxidative stress in HepG2 cells

Given that HepG2 cells grown in iron-rich media developed iron overload (Figs 1D and 2A) and excess iron is known to catalyze oxidative reactions harmful to the cell, we examined parameters of oxidative stress, namely the intracellular production of reactive oxygen species (ROS) by using the probe 2′,7′-dichlorodihydrofluorescein (DCFH). In preliminary experiments, it was observed that the basal levels of fluorescence in HepG2 cells labeled with DCFH-diacetate (DA) and cultured for 1–24 h were very high when compared to other cell types such as resting T cells (data not shown). In subsequent experiments, ROS production was determined after the short incubation period with DCFH-DA. As shown in Fig. 2B (thin line), HepG2

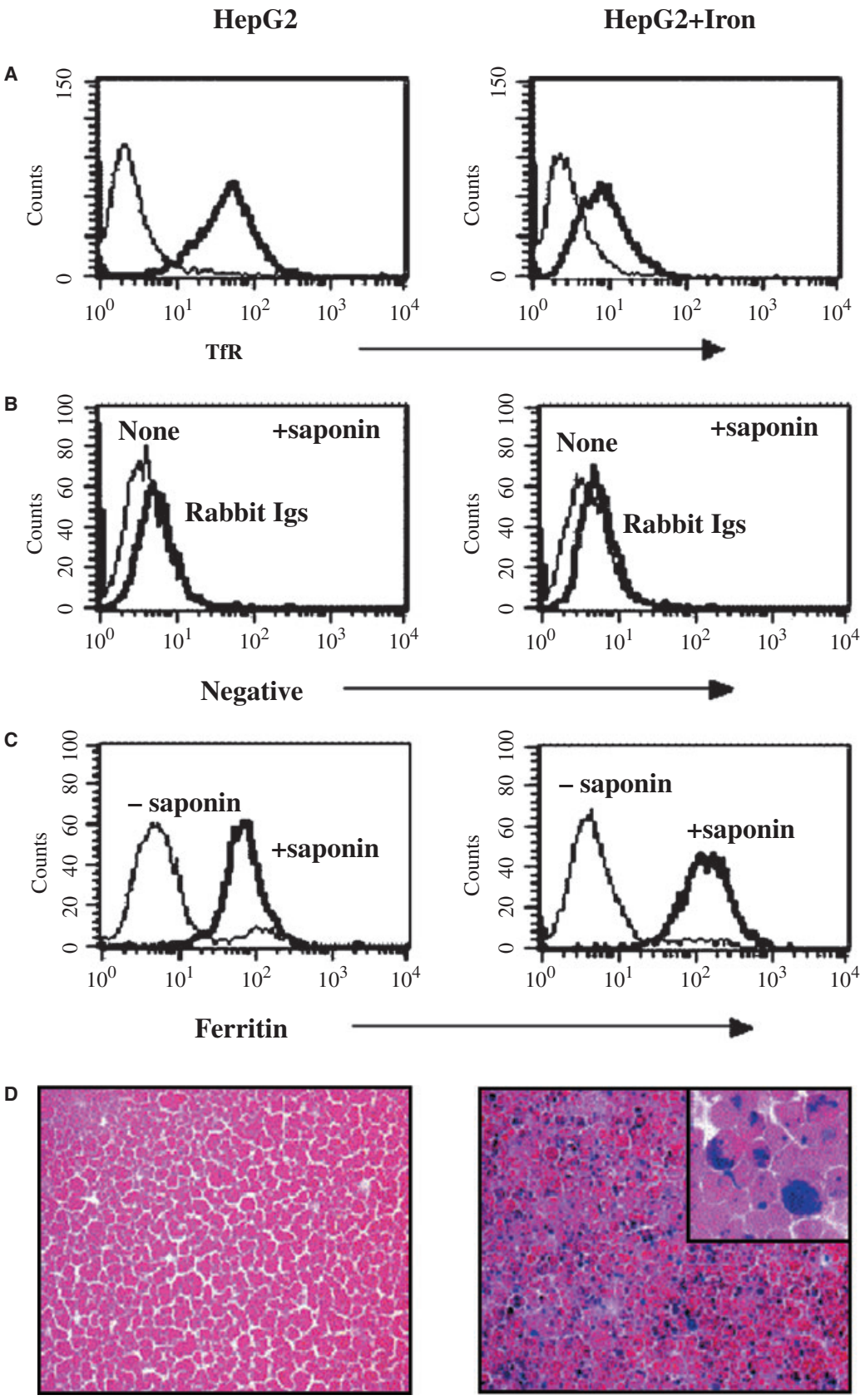
HepG2
HepG2+Iron
A
Counts
150
0
10^0 10^1 10^2 10^3 10^4
TfR
B
None
+saponin
Rabbit Igs
0 20 40 60 80 100
Negative
C
– saponin
+saponin
Ferritin
D

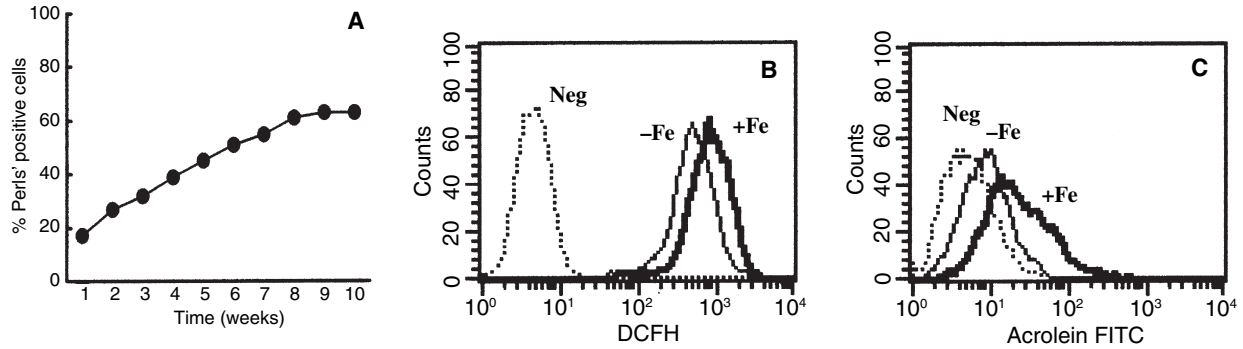

Fig. 2. Kinetics of iron-loading and oxidative stress parameters in iron-loaded HepG2 cells. HepG2 cells were cultured for 1–10 weeks in the absence or presence of 100 μM of ferric citrate. (A) Kinetic study showing the percentage of Perls' positive HepG2 cells with time of culture in iron-rich media. A total of 200 cells were counted in each time point. (B) For ROS determination growing cells were first incubated with 10 μM of DCFH-DA, harvested and acquired immediately in a FACSCalibur and analyzed using the CELLQUEST software. Histogram shows DCFH fluorescence in HepG2 cells grown without (thin line, – Fe) or with (thick line, + Fe) iron in one representative of five separate experiments. Dotted line represents background staining in HepG2 cells not loaded with DCFH-DA. (C) For determination of oxidatively modified proteins, cells were harvested and stained with 5F6 (anti-acrolein) followed by FITC-conjugated rabbit anti-(mouse Igs). Cells were acquired immediately in a FACSCalibur and analyzed using CELLQUEST. Histogram shows cell surface expression of acrolein adducts in HepG2 cells cultured without (thin line, – Fe) or with (thick line, + Fe) iron. Dotted line represents background staining with mouse Igs as the first-step antibody. One representative of seven separate experiments is shown.

cells cultured in normal media naturally produced ROS at high levels as indicated by the high mean fluorescence intensity when compared to background staining in unlabeled cells or resting T cells (data not shown). Yet, HepG2 cells grown in iron-rich media showed a further increase in ROS production as determined by an increase in DCFH mean fluorescence intensity (Fig. 2B, thick line). In addition, determination of acrolein adducts, a marker of oxidative stress in biological systems [25], on the cell surface of HepG2 cells by flow cytometry revealed that HepG2 cells have low but detectable levels of acrolein adducts and that culture in iron-rich media induces a marked increase (Fig. 2C).

Fig. 1. Regulation of iron related parameters by iron loading in HepG2 cells. HepG2 cells were cultured in normal media or media supplemented with 100 μM of ferric citrate for 4–8 weeks. Cells were stained with Ber-T9 monoclonal antibodies (anti-CD71) and rabbit anti-ferritin Igs, followed by FITC-conjugated rabbit anti-mouse and FITC-conjugated swine anti-rabbit Igs, respectively. Mouse and rabbit Igs were used as control to define background staining. For intracellular staining, cells were first permeabilized with 0.2% saponin. Labeled cells were acquired in a FACSCalibur and analyzed using the CELLQUEST software. (A) Histograms show cell surface expression of the transferrin receptor (thick lines) in nonpermeabilized cells cultured without and with iron. Thin lines represent background staining with mouse Igs. (B) Histograms show background staining with no antibody (thin lines) or with rabbit Igs (thick lines) as first step in permeabilized cells. (C) Histograms show ferritin expression in nonpermeabilized (thin lines, – saponin) and permeabilized cells (thick lines, + saponin) cells cultured without and with iron as indicated. (D) Perls' staining of cytospins of HepG2 cells grown in media supplemented with 100 μM of ferric citrate for 8 weeks showing iron accumulation (blue) in HepG2 cells at ×100 original magnification. Inset shows a ×400 original magnification. One representative of at least three separate experiments is shown.

HepG2 cells grown in iron-rich media show growth retardation but not increased cell death

To ascertain whether the increase in oxidative stress parameters observed in HepG2 cells cultured in iron-rich media had any impact on viability and/or cell growth, cell recovery at the end of the weekly culture periods was determined. Recovery of viable HepG2 cells cultured with iron-rich media was significantly reduced when compared with cells cultured in normal media (Fig. 3A). However, quantification of nonviable cells (trypan blue positive) demonstrated that the decrease in cell recovery was not due to an increase in cell death (Fig. 3A). Quantification of DNA content by flow cytometry revealed that the inhibition of cell growth was due to a decrease in the percentage of cells in the S and G2/M phases of the cell cycle (Fig. 3B). In a total of seven separate determinations, a statistically significant decrease in the percentage of dividing HepG2 cells (S + G2/M) was observed in the iron-rich cultures ($P = 0.017$, Fig. 3B). In accordance with the cell viability studies, growth retardation in HepG2 cells cultured in iron-rich media was not associated with an increase in the percentage of apoptotic cells

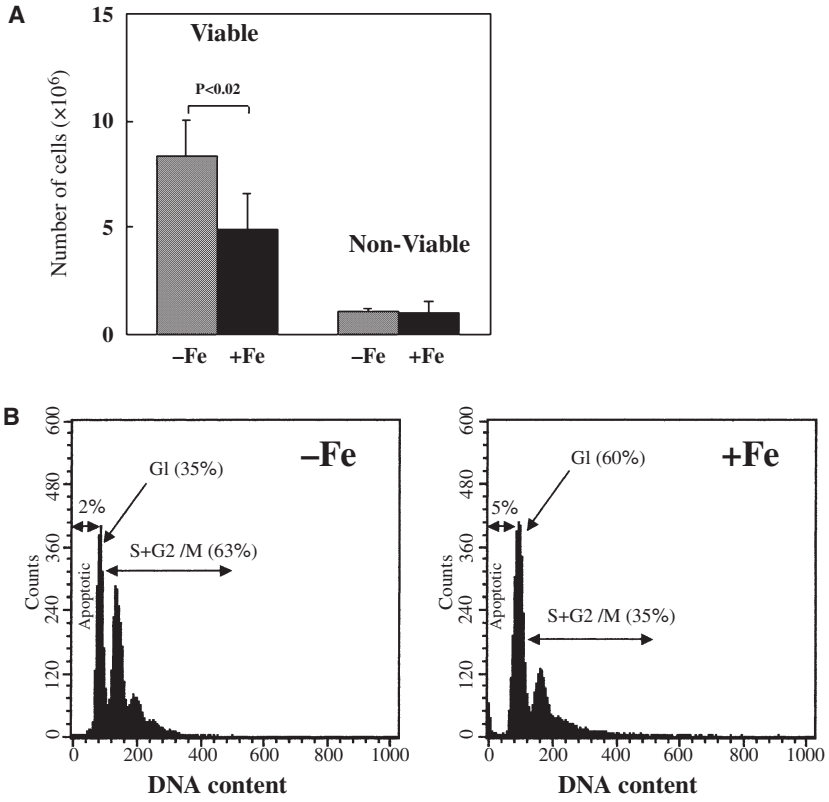

Fig. 3. Iron-rich media inhibits growth of HepG2 cells. HepG2 cells were cultured in normal media or media supplemented with 100 μM of ferric citrate for 4–8 weeks. After harvesting, total viable and nonviable cells, as determined by trypan blue exclusion and inclusion, respectively, were counted using a hematocytometer. After extensive washing, cells were evaluated for DNA content in a FACSCalibur as indicated in the Methods. (A) Bars show the number of viable and nonviable HepG2 cells (mean ± SD, $n = 8$) after culture in media without (– Fe) and with (+ Fe) iron. Statistically significant differences (Student's *t*-test) are indicated. (B). Histograms show the percentage of apoptotic cells (subG0/G1), and cells into the G1 and S + G2/M phases in the two culture conditions. One representative of at least five separate experiments is shown.

(subG0/G1), but with an increase of cells in G1 phase, i.e. an increase in cell arrest (Fig. 3B).

Expression of immunoregulatory molecules by HepG2 cells

Next, we examined the expression of cell surface molecules involved in immune activation and recognition. HepG2 cells grown in normal media displayed moderate to high levels of ICAM-1, gp180 and MHC class I molecules on the cell surface. CD1d, as recognized by Nor3.2 antibodies, was expressed at very low levels and MHC class II molecules barely detectable (Fig. 4A). Culture of HepG2 cells in iron-rich media induced a significant increase in the percentage of HepG2 cells expressing Nor-3.2-reactive CD1d, while the expression of ICAM-1, gp180 and MHC molecules was not affected significantly (Fig. 4A). On average, a twofold increase in the percentage of CD1d + cells was observed in HepG2 cells grown in iron-rich media ($P < 0.001$, $n = 9$). As Nor3.2 was generated by immunizing mice against a recombinant denatured CD1d protein the capacity of this antibody to recognize native CD1d molecules is limited [26]. Accordingly, further studies were performed using CD1d42 antibodies, which recognize native CD1d. In contrast to Nor3.2-reactive molecules, CD1d42-reactive molecules were absent from the cell surface of HepG2 cells and culture in iron-rich media did not influence their expression (Fig. 4B).

CD1d protein and mRNA are upregulated in iron-loaded HepG2 cells

Immunocytochemistry and immunofluorescence studies confirmed that Nor3.2-reactive CD1d is expressed by a low percentage of HepG2 cells, mainly in the cytoplasm, while CD1d expression by HepG2 cells grown in iron-rich media showed a preferential localization into proximal regions of the plasma membrane (Fig. 5A). The increase in CD1d expression at the cell surface was confirmed by immunoprecipitation studies. Nor3.2 immunoprecipitates from lysates of cell surface biotinylated HepG2 cells, grown in iron-rich media, showed a major band of 90–95 kDa that corresponded to the expected molecular mass of dimers of mature glycosylated CD1d molecules; this was about threefold higher than the band immunoprecipitated from lysates of HepG2 cells cultured in normal media (Fig. 5B). Western blotting analysis of immunoprecipitates from nonbiotinylated lysates and mRNA measurements by RT-PCR revealed that the

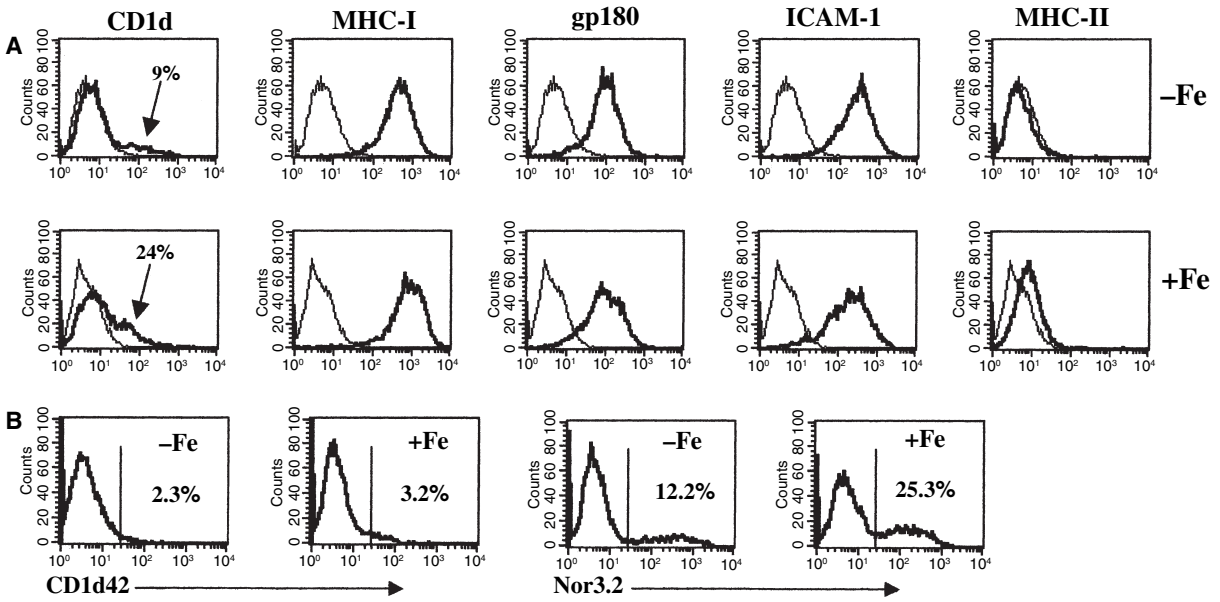

Fig. 4. Upregulation of CD1d molecules at the cell surface of iron-loaded HepG2 cells. HepG2 cells were cultured in normal media or media supplemented with 100 μM of ferric citrate for 4–8 weeks. After harvesting, cells were stained with mouse monoclonal antibodies against CD1d (Nor3.2 and CD1d42), MHC class I (W6/32), gp180 (B9), ICAM-1 (MCA534), and MHC class II (CR3/43), followed by FITC-conjugated rabbit anti-(mouse Igs) (thick lines). Mouse Igs were used to define background staining (thin lines). Cells were then acquired in a FACScalibur and analyzed using CELLQUEST. (A) Histograms show the expression of the molecules studied in HepG2 cells cultured in the absence (– Fe) or presence (+ Fe) of iron in a representative experiment of at least nine different determinations, with the exception of CR3/43 (n = 3). (B) Histograms compare the levels of expression of Nor3.2-reactive and CDd142-reactive CD1d molecules in HepG2 cells cultured in the absence (– Fe) or presence (+ Fe) of iron in a representative experiment out of three different determinations.

marked increase in CD1d at the cell surface of iron-loaded HepG2 cells was paralleled by an increase on the total CD1d protein and mRNA, although not of the same magnitude (Fig. 5B,C). Although HepG2 cells cultured in the presence of ferric citrate showed features of iron accumulation (Fig. 1) and oxidative stress (Fig. 2) concomitant with an increase in the percentage of CD1d+ positive cells [Fig. 4], the latter effect could not be attributed to oxidative stress *per se*. Indeed, oxidants such as H_2O_2 and diamide applied exogenously were incapable of reproducing the results obtained with ferric citrate. Rather, these oxidants induced cell death of HepG2 cells (data not shown).

Upregulated CD1d expression and alterations in lipid parameters

Considering that CD1d is an unconventional MHC class I molecule specialized in binding lipids and is proposed to monitor lipid membrane integrity [27], we studied changes in membrane lipid composition and intracellular lipid content in HepG2 cells by examining phosphatidylserine expression and lipid droplet accumulation, respectively. Phosphatidylserine is a lipid that is enriched in the inner face of the plasma membrane and that is translocated into the outer face under certain cellular states. Double-labeling with Annexin V and CD1d revealed that a large number of HepG2 cells growing in normal media already expressed phosphatidylserine in the plasma membrane with a third of these cells also expressing CD1d (Fig. 6A, left dot-plot). Interestingly, the increase in phosphatidylserine expression by HepG2 cells grown in iron-rich media was of the same order of magnitude as the upregulation of CD1d expression (Fig. 6A, right dot-plot). Immunofluorescence experiments indicated that phosphatidylserine and Nor3.2-reactive CD1d molecules colocalize in the plasma membrane of HepG2 cells (data not shown). To ascertain whether phosphatidylserine translocation was associated with changes in intracellular lipid metabolism, we examined lipid content in iron-loaded HepG2 cells by Oil Red staining. Faint lipid accumulation was observed in HepG2 cells grown in normal media (Fig. 6B). In marked contrast, culture in iron rich-media induced a manifest increase in lipid accumulation in HepG2 cells (Fig. 6B). Electron microscopy studies confirmed that iron-loaded HepG2 cells showed many lipid droplets (Fig. 6C).

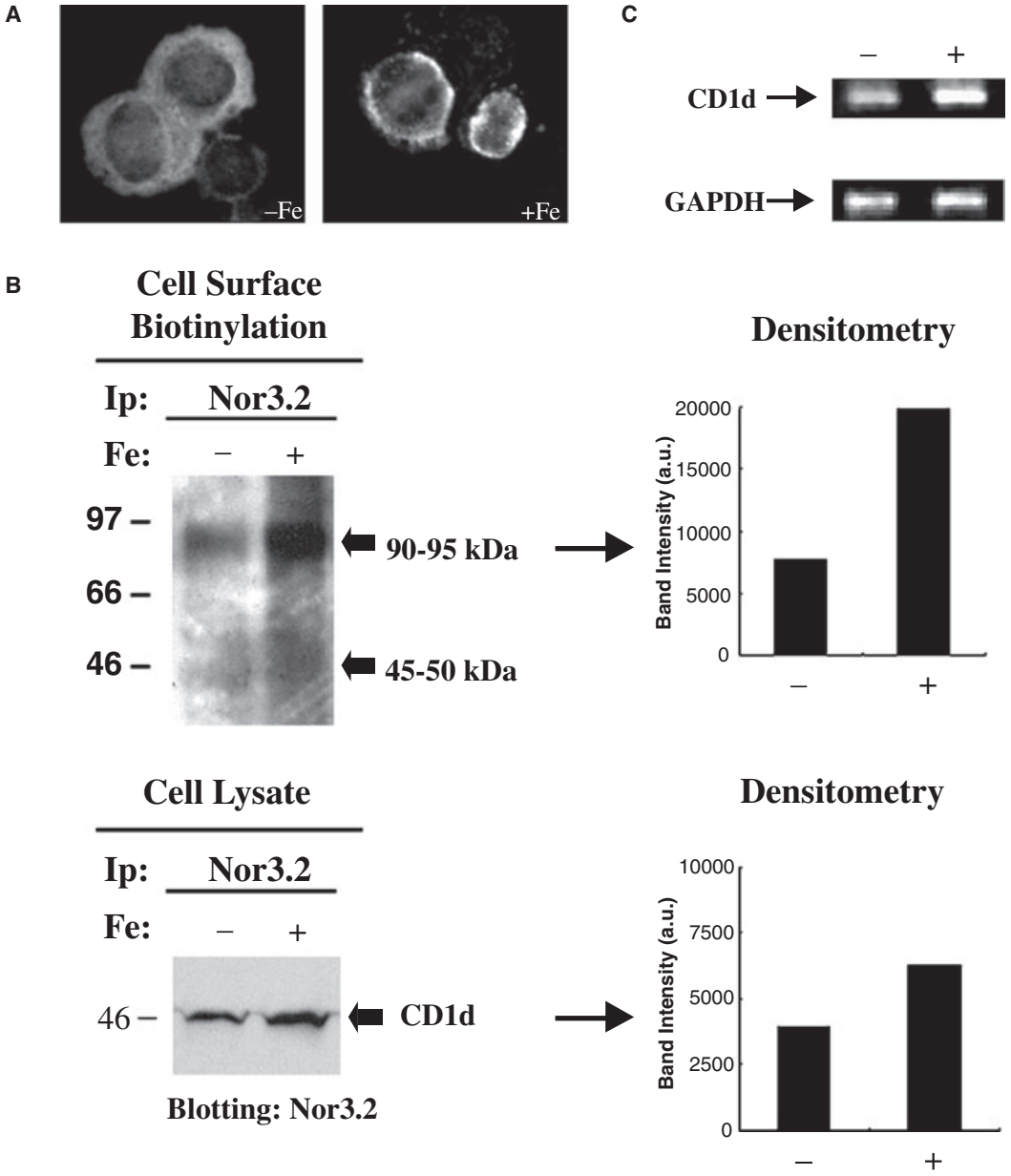

Fig. 5. Iron-induced upregulation of cell surface CD1d is accompanied by an increase in total protein and mRNA transcripts. HepG2 cells were cultured as indicated in legend of Fig. 1 and cells processed for immunocytochemistry, immunoprecipitation and mRNA studies. (A) Cytospins of HepG2 cells were incubated with Nor3.2 followed by rabbit anti-(mouse Igs) and the alkaline phosphatase-antialkaline phosphatase (APAAP) conjugate, as described in Methods. Color was developed with Fast-Red substrate. Images showing CD1d expression in HepG2 cells grown in media without (– Fe) and with (+ Fe) iron were taken in an Axioskop microscope equipped with a SPOT II camera. (B) Lysates corresponding to 5×10^6 biotinylated (upper panel) and nonbiotinylated (lower panel) HepG2 cells grown in media without (–) and with (+) iron were immunoprecipitated with Nor3.2 antibodies. Biotinylated and nonbiotinylated samples were boiled in 1% SDS and separated on a 10% SDS/PAGE under nonreducing and reducing conditions, respectively, and proteins transferred to nitrocellulose filters. Cell surface biotinylated CD1d molecules were visualized by using Super-Signal West Femto (Perbio). CD1d dimers (90–95 kDa) and monomers (45–50 kDa) are indicated. Non-biotinylated total CD1d molecules were visualized after immunodetection with Nor3.2 followed by HRP-conjugated rabbit anti-(mouse Igs) and Super-Signal West Femto (Perbio). Densitometry quantification of the CD1d protein bands indicated was performed using a Kodak Digital Science DC40 camera and its associated software. Band intensities are shown on the right and are expressed as the sum of all pixel intensity values in the band rectangle. (C) RT-PCR of total RNA isolated from HepG2 cells grown in normal media (–) or media supplemented with 100 μM of ferric citrate (+). Primers specific for CD1d and GAPDH were used as described.

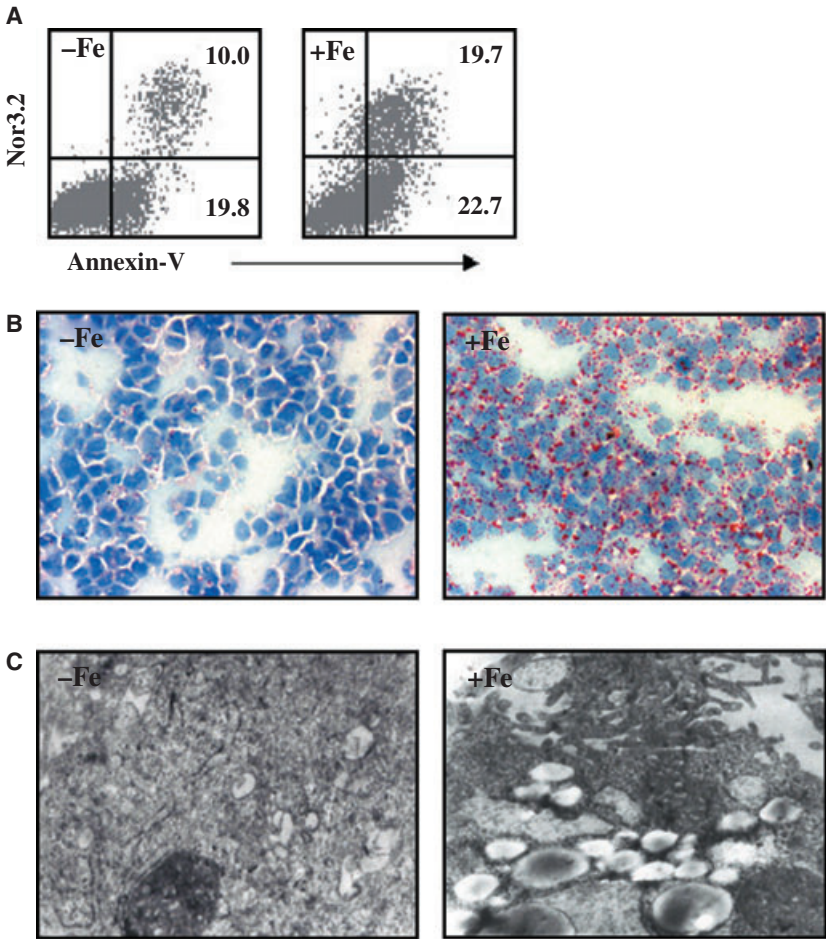

Fig. 6. Alterations in lipid metabolism parameters in iron-loaded HepG2 cells. HepG2 cells were cultured for 4 weeks as indicated in legend of Fig. 1 and processed for flow cytometry, immunocytochemistry and transmission electron microscopy as indicated in the Methods. (A) Four-log dot-plots show double-labeling of CD1d (FL-2) and phosphatidylserine (FL-1) in HepG2 cells cultured without (– Fe) or with (+ Fe) iron. The percentage of HepG2 cells positive for phosphatidylserine (lower right quadrant) and phosphatidylserine plus CD1d (upper right quadrant) in each culture condition is indicated. (B) Pictures show Oil Red O staining of cryostat sections of HepG2 cells cultured without (– Fe) or with (+ Fe) iron and counterstained with hematoxylin at ×200 original magnification. (C) Pictures show TEM images of sections of HepG2 cells cultured without (– Fe) or with (+ Fe) iron at ×16 000 original magnification.

Discussion

In the human liver CD1d molecules are expressed mainly in the cytoplasm [21]. Herein we have shown that iron loading of HepG2 cells, a hepatocytic cell line, resulted in increased cell surface expression of CD1d molecules recognized by Nor3.2 but not by CD1d42 antibodies. Interestingly, CD1d42 antibodies recognize the native 'folded' CD1d molecule, while Nor3.2 antibodies recognize non-native CD1d molecules [26]. However, CD1d upregulation was not paralleled by a significant increase in gp180, a heavy glycosylated protein that associates with CD1d in epithelial cells [28], or in other immune recognition ligands such as classical MHC class I and II molecules and ICAM-1. Studies by Hultcrantz and colleagues reported that upregulation of ICAM-1 expression by hepatocytes in hereditary hemochromatosis only takes place in patients with Kupffer cell iron overload [13]. Thus, it is probable that hepatic iron loading, as the reported in this study using HepG2 cells, is unable *per se* of regulating the expression of ICAM-1, and other immune recognition molecules other than Nor3.2-reactive CD1d.

To our knowledge, iron loading does not regulate members of the MHC class I family. For instance, conflicting results have been reported regarding the expression of HFE by human intestinal cells. While Han *et al.* reported that expression of HFE was regulated by iron load, in another study, Tallkvist *et al.* found that iron overload had no effect on HFE [29,30]. Probably, changes in the expression of HFE protein under iron overload conditions are secondary to changes in proteins known to interact with molecules of the MHC family. In this context, it is important to draw attention to the fact that HepG2 cells grown in iron rich media: (a) induced coordinated changes in the expression of the transferrin receptor and ferritin; (b) developed iron accumulation and (c) increased the prooxidant state and the level of oxidatively modified proteins. These results are in accordance with previous *in vitro* and *in vivo* studies of hepatic iron loading [31–35]. Evidence for toxicity

caused by excess of iron in the liver is now well established and there is evidence that the harmful effect of iron accumulation is due to the prooxidant state created that is preceded by an increase in the labile iron pool [34–37]. By using the ROS detector probe DCFH we have shown that basal level of oxidative stress in HepG2 cells is already high and that is exacerbated by growth in iron-rich media. We have also shown that the increase in the prooxidant state caused by iron loading has an impact in protein integrity, as indicated by an increase in protein-bound acrolein adducts at the cell surface, which point to acrolein-adducts as a reliable marker of lipid peroxidation also in iron overload disorders [25]. Most importantly, the changes in parameters of oxidative stress caused by iron in HepG2 cells were associated with growth retardation due to a decrease in the percentage of cells in the cycle with concomitant cell arrest in the G1 phase. Overall, and considering that in clinical situations of iron overload fibrosis is associated with proliferation of stelleate cells and synthesis of collagen [36,37], the *in vitro* data presented here may be relevant for understand some of the complex mechanisms responsible for the development of fibrosis and cirrhosis *in vivo*.

A number of intracellular pathways activated in iron-loaded HepG2 cells as a result of the undergoing metabolic changes observed might have resulted in the activation of *CD1d* gene expression and a subsequent increased expression. Indeed, RT-PCR experiments showed an increase in *CD1d* mRNA levels in iron-loaded HepG2 cells. Yet, the combination of the flow cytometry and immunoprecipitation data suggests that the increase in CD1d molecules at the cell surface could not be solely the result of increased transcription but also from intracellular redistribution. In this scenario, it is tempting to speculate that the appearance of Nor3.2-reactive CD1d molecules at the cell surface of iron-loaded HepG2 cells could be a consequence of CD1d misfolding in intracellular compartments with a subsequent release of the bound lipid; thus altering the intracellular lipid content. A number of previous studies tend to support this view. First, CD1d has a conserved tyrosine motif within its cytoplasmic tail that permits the association with molecules that facilitate trafficking between the plasma membrane and endolysosomal compartments [38–40]. Second, earlier studies showed that in situations of hepatic iron loading, iron accumulates primarily in lysosomes leading to alterations in membrane composition and vesicular pH [41–43]. Third, CD1d has the capacity to bind a variety of intracellular lipids in the endolysosomal compartment and changes in the pH of these compartments may alter lipid binding by CD1d molecules and, consequently, trafficking between the plasma membrane and endolysosomes [44].

Taking into consideration these studies, upregulation of CD1d in iron-loaded HepG2 cells could be largely due to biochemical and molecular changes that take place within the endolysosomal compartment and that result in a redistribution of endolysosomal CD1d molecules to the plasma membrane. Interestingly, in the present study we demonstrated that iron-loading of HepG2 cells led to marked changes in lipid metabolism. Thus, expression of phosphatidylserine at the outer part of iron-loaded HepG2 cells was increased, and double-labeling revealed that the increase in phosphatidylserine expression was of the same order of magnitude as the upregulation of CD1d expression. In other words, the same HepG2 cells expressed CD1d and phosphatidylserine. Although phosphatidylserine externalization is regarded as a hallmark of apoptosis, recent studies suggest that phosphatidylserine expression, and membrane lipid redistribution in general, is a normal event in viable cells that marks a process related with the cell cycle status [45]. In this context, it is important to stress that DNA content studies did not show significant differences in apoptosis (subG0/G1) between normal and iron-loaded HepG2 cells. Further examination of lipid metabolism parameters led to the finding of overt lipid accumulation and lipid droplet formation in iron-loaded HepG2 cells, as verified by Oil Red O staining and transmission electron microscopy. These data reinforce the view that changes in lipid metabolism take place in iron loaded HepG2 cells which may underlie the redistribution of CD1d and its expression at the cell surface. A study showing that CD1d expression augments in lipid-laden macrophages from atherosclerotic tissue supports this view [46].

Apart from the present study, Nor3.2-reactive CD1d has been found altered in keratinocytes from psoriatic lesions [47], in the gastrointestinal tract of certain inflammatory diseases [48,49], and in primary biliary cirrhosis [50]. Whether iron and/or lipid metabolism are altered in any of these conditions is not known. In our view, upregulation of CD1d molecules at the cell surface of iron-loaded HepG2 cells in a non-native form may have implications at two different levels; at the level of the hepatic cell itself and at the level of the relationship with neighboring cells. At the level of the hepatocyte, CD1d redistribution may influence quantitatively and qualitatively the intracellular lipid pool by either intracellular release and/or extracellular uptake. At the level of the relationship with adjacent cells *in vivo*, upregulation of CD1d by hepatocytes may function as a signaling device that activates selected subsets of resident NK CD8+ T cells (reviewed in

[51]). Recent studies in humans during hepatitis C viral infections showing that hepatic CD1d is upregulated and recognized by CD1d-specific T cells tend to support this assumption [52]. Activation of CD1d-restricted T cells may induce the secretion of cytokines capable of regulating hepatic iron metabolism [53]. Alternatively, phosphatidylserine expression, concomitant with CD1d, by iron-loaded hepatocytes may facilitate phagocytosis and removal of the purportedly apoptotic cells by resident macrophages through the phosphatidylserine receptor [54]. Removal of apoptotic cells may avoid local inflammation by a number of different mechanisms, such as production of TGF-β1 as seen in iron-overloaded hemochromatosis patients [33]. TGF-β1 production under iron overload could be the result of the phosphatidylserine/CD1d-dependent ingestion of apoptotic hepatocytes by resident Kupffer cells and may contribute to reduce local inflammation, as demonstrated in a recent report [55].

The present *in vitro* model may be used to study mechanisms of hepatic cell function under a number of stressful conditions associated with iron-overload, such as viral infections or heavy alcohol consumption and to examine the possible role played by cells and molecules of the immunological system in hepatic injury and repair. Understanding the interdependence between the metabolism of iron and lipids [14,56,57] may be relevant in a variety of liver diseases. It is anticipated that iron overload in hepatic cells in clinical situations *in vivo* might cause changes in lipid metabolism and consequently in lipid binding molecules such as CD1d.

Materials and methods

Cells and culture conditions

The hepatocellular carcinoma cell line HepG2 was purchased from the European Collection of Cell Cultures (ECACC, Wiltshire, UK) and maintained in Minimum Essential Medium, MEM (Gibco, Invitrogen, Merelbeke, Belgium) supplemented with 1% (w/v) antibiotic/antimiotic solution (Sigma-Aldrich, Barcelona, Spain), 1% (w/v) glutamine, 1% (w/v) nonessential amino acids and 2% (w/v) fetal bovine serum (Biochrom KG, Berlin, Germany). Paired cultures of cells growing in normal media or in iron-rich media were set up and maintained for different periods of time as indicated. Iron-rich media consisted of MEM supplemented with 100 μM of ferric citrate (Sigma-Aldrich). Ferric citrate was prepared freshly from a stock solution of 25 mM made in distilled H_2O by gentle agitation at 65 °C and stored at 4 °C. Unless otherwise indicated, cells were seeded at 2×10^6 per 75-cm^2 flask (TPP, Trasadingen, Switzerland) and stored for a week in an incubator at 37 °C, 5% (v/v) CO_2 and 99% humidity. After this period, cells were treated with a solution of 1% (w/v) trypsin/EDTA (Gibco), washed with Hanks' balanced salt solution (HBSS), counted and replated as described above. HepG2 cells cultured in MEM-2% usually reached confluence with a viable cell recovery between 7 and 9×10^6 cells per flask during the 1-week period. To analyze the effect of direct oxidative stress, HepG2 cells were grown in the presence of H_2O_2 and diamide (Sigma-Aldrich). Seven days after, phenotypic and morphological parameters of cell growth and survival were determined.

Flow cytometry

Approximately 0.3×10^6 cells were cell surface stained with the appropriate antibodies in staining solution [NaCl/P_i, 0.2% (w/v) BSA, 0.1% (w/v) sodium azide] and analyzed in a FACScalibur (Becton Dickinson, Mountain View, CA, USA). For intracellular staining, fixed cells in 2% (v/v) formaldehyde were first permeabilized by incubation in NaCl/P_i/0.2% (w/v) saponin for 10 min. The following primary antibodies were used: W6/32, a monoclonal antibody to human β2m-associated MHC class I molecules (DAKO, Glostrup, Denmark); CR3/43, a monoclonal antibody to human MHC class II molecules (DAKO); Nor3.2 a monoclonal antibody to non-native human CD1d (BIODESIGN, Saco, ME, USA [26]); CD1d42, a monoclonal antibody to native human CD1d (Pharmingen, San Diego, CA, USA); 1B9, a monoclonal antibody to the human intestinal epithelial molecule gp180 (a gift from L. Mayer, Mount Sinai School of Medicine, New York, USA); MCA534, a monoclonal antibody to human ICAM-1 (SEROTEC, Oxford, UK); Ber-T9, a monoclonal antibody to the human transferrin receptor (DAKO); rabbit Igs to human ferritin (DAKO); 5F6, a monoclonal antibody to oxidatively modified proteins containing the aldehyde adduct acrolein (a gift from K. Uchida, Nagoya University, Nagoya, Japan). Rabbit anti-mouse and goat anti-rabbit Igs, fluorescein isothiocyanate (FITC) or R-phycoerythrin-conjugated, were from DAKO. Mouse and rabbit Igs (DAKO) were used as negative controls. Annexin V-FITC was from BD Biosciences (San Diego, CA, USA).

Determination of intracellular iron

Intracellular ferric iron was detected by the Perls' Prussian blue. Briefly, cytospins (centrifugations of cell suspensions on glass slides) of HepG2 cells were fixed and incubated for 1 h in a 1 : 1 solution of 2% potassium ferrocyanide/2% HCl (w/v/v). Afterwards, cytospins were rinsed in distilled water, counterstained with erytrosin, dehydrated in 70% (v/v) alcohol, then in 100% (v/v) alcohol and xylol, and finally mounted in Entellan (Merck, Barcelona, Spain).

Determination of phosphatidylserine expression and cell death

Phosphatidylserine expression on the outer part of the plasma membrane was examined by Annexin V binding. Briefly, cells were washed twice with binding buffer (10 mM Hepes, 140 mM NaCl and 2.5 mM $CaCl_2$, pH 7.4) and incubated with Annexin V-FITC for 15 min at room temperature. Cells were analyzed immediately by flow cytometry. In immunofluorescence studies, cells were fixed in acetone prior to analysis. Cell death was determined by trypan blue staining. Aliquots of HepG2 cells were resuspended in NaCl/P_i containing trypan blue. Dead and alive cells were counted in a NEUBAUER chamber under a light microscope.

Measurement of oxidative stress and DNA content

Oxidative stress was measured through the detection of ROS and of protein-bound acrolein. ROS produced within HepG2 cells were detected with the membrane permeant probe 2′,7′-dichlorodihydrofluorescein-diacetate (DCFH-DA). ROS produced by the cell oxidize DCFH to DCF, which after excitation at 488 nm, emits fluorescence at 530 nm (FL-1 channel). Growing HepG2 cells were incubated with 10 μM of DCFH-DA in culture media for 30 min at 37 °C and washed three times with the same media. Cells were then harvested and analyzed immediately by flow cytometry. Protein-bound acrolein was detected by flow cytometry after labeling with the mouse monoclonal antibody 5F6, followed by the appropriate fluorochrome-conjugated rabbit anti-mouse Igs. To evaluate DNA content, HepG2 cells were permeabilized with ice-cold 70% (v/v) ethanol for 10 min. Then, cells were washed three times with NaCl/P_i and stained for 30 min at 37 °C with 50 $\mu g \cdot mL^{-1}$ of propidium iodide in NaCl/P_i. Labeled cells were acquired immediately in a FACScalibur and apoptotic (subG0/G1), resting (G1) and dividing (S + G2/M) cells determined by DNA content (PI fluorescence) monitored on the FL-3 channel.

Cell labeling, immunoprecipitation and immunoblotting

For immunoprecipitation of cell surface CD1d, HepG2 cells were incubated with 0.5 $\mu g \cdot mL^{-1}$ of NHS-sulfo-biotin (Perbio Science, Cheshire, UK) in NaCl/P_i for 10 min at room temperature (20–25 °C) followed by four washes in NaCl/P_i. After washing, labeled cells were lysed in lysis buffer [20 mM Tris pH 7.6, 150 mM NaCl, 1 mM phenylmethanesulfonyl fluoride and 1% (v/v) Triton X-100] for 30 min on ice. The lysates were centrifuged at 10 000 ***g*** to remove cell debris and precleared for 1 h with protein-A Sepharose beads (Amersham Pharmacia Biotech, Buckinghamshire, UK). Precleared detergent lysates were boiled for 10 min in 0.1% (v/v) SDS and then immunoprecipitated with Nor3.2 and protein A-Sepharose beads for 2 h at 4 °C. Washed immunoprecipitates were boiled for 5 min and resolved by SDS/PAGE. Proteins were blotted onto nitrocellulose membranes (Amersham Pharmacia Biotech) and the filters blocked with 5% (w/v) nonfat dry milk in TBS-T. Washed filters were incubated for 1 h with a 1 : 7500 dilution of streptavidin-conjugated horseradish peroxidase (Sigma) in TBS-T, and proteins visualized using Super Signal (Perbio Science). For detection of total CD1d molecules, cell lysates of nonbiotinylated cells were immunoprecipitated, resolved by SDS/PAGE and transferred onto nitrocellulose membranes as above. Afterwards, filters were incubated with Nor3.2 antibodies for 1 h in TBS-T, followed by incubation with HRP-conjugated goat anti-(mouse Ig) Igs (Molecular Probes, Leiden, the Netherlands). After extensive washing, CD1d was visualized with Super Signal (Perbio Science).

RT-PCR

HepG2 cells were collected into cryotubes vials (Nunc, VWR International, Lisbon, Portugal), snap frozen in liquid nitrogen and stored at −70 °C for further analysis. From each sample, total RNA was isolated and DNAse treated using the RNeasy kit according to the manufacture specifications (Qiagen, Victoria, Australia). The total RNA concentration was measured by spectrophotometer and its quality assessed by agarose gel electrophoresis. Subsequently, 5 μg of total RNA was converted into cDNA by using the termoscript RT-PCR system (Gibco) according to the recommended protocol. The *CD1d* gene was amplified by PCR using the following primers: 5′-GGGCACTC AGCCAGGGGACATCCTGCCCAA-3′ as forward and 5′-GATACAAGTTTGCACACCTTTGCACTTCTG-3′ as reverse [58]. The PCR amplification was performed in a total volume of 50 μL reaction mix containing 1 μL of cDNA, 10 pmol of each primer, 10× reaction buffer, 0.5 mM dNTPs and 2 units of *Taq* polymerase (Promega, Madison, WI, USA). For the CD1d amplification, we used the following PCR program: an initial denaturing step of 3 min at 92 °C, followed by 35 cycles (92 °C for 30 s, 55 °C for 1 min and 72 °C for 3 min) and a final extension step for 10 min at 72 °C. Subsequently, 10 μL of the PCR products were loaded into a 1.5% agarose gel with 1× ethidium bromide, the electrophoresis performed and the 547 bp fragment visualized under UV light. To ensure that the cDNA samples were of similar concentration and quality, the *GAPDH* gene was also amplified by using a similar protocol with the housekeeping gene specific primers: 5′-CCATGGAGAAGGCTGGGG-3′ as forward and 5′-CA AAGTTGTCATGGATGACC-3′ as reverse.

Immunocytochemistry and immunofluorescence

Cytospins of HepG2 cells in poly(L-lysine)-coated slides (Sigma) were air-dried and fixed with 100% (v/v) acetone. Immunocytochemistry was performed by using the alkaline phosphatase-antialkaline phosphatase (APAAP) method. Briefly, cytospins were incubated with normal rabbit serum diluted 1 : 10 for 10 min. Then, cells were incubated with Nor3.2 or with DAK-GO1 a monoclonal antibody of the same isotype but specific for *Aspergillus niger* glucose oxidase (negative control). After washing, cytopins were incubated with rabbit anti-mouse Igs for 30 min, followed by a further 30 min with the APAAP conjugate. These steps were repeated for 10 min each to increase the intensity of the signal. After three additional washes, color was developed with Fast-Red substrate. Reagents were from DAKO. Preparations were analyzed on an Axioskop microscope (Zeiss, Göttingen, Germany) equipped with a SPOT II camera (Diagnostic Instruments, Sterling, Michigan, USA). For immunofluorescence studies, the tyramide signal amplification TSA kit containing a HRP-conjugated secondary antibody and Alexa 568-labeled tyramide was used (Molecular Probes, Leiden). Briefly, cells were first stained in suspension with Nor3.2 followed by HRP-goat anti-(mouse IgG). For phosphatidylserine determination, cells were washed with binding buffer and incubated with Annexin V-FITC for 15 min at room temperature. Cells were deposited immediately in poly(L-lysine) coated slides and incubated with Alexa Fluor 568 tyramide following manufacturer instructions. Preparations were fixed in 100% acetone at −20 °C for 5 min, mounted in Vectashield with 4′,6-diamidino-2-phenylindole (DAPI) (Vector Laboratories, Inc., Burlingame, CA) and analyzed in an Axioskop microscope (Zeiss).

Electron microscopy

The ultrastructure of HepG2 cells was examined by transmission electron microscopy following established routine protocols. Briefly, HepG2 cells were harvested after trypsin treatment, washed extensively and fixed in 2.5% (v/v) glutaraldehyde in cacodylate buffer (0.1 M, pH 7.2) and post-fixed in 1% (w/v) osmium tetroxide in the same buffer. The samples were then embedded in Epon resin (TAAB Laboratories Equipment Ltd, Berkshire, UK) after dehydration in a series of graded ethanol. Ultrathin sections were cut with an RMC MT-7 microtome and contrasted with uranyl acetate and lead citrate. Observations and micrographs were performed under a Zeiss EM10 electron microscope.

Microscopic evaluation of lipid droplets

Light microscopic examination of lipid droplet was performed using Oil Red O. HepG2 cells were harvested after trypsin treatment and washed extensively. Then, cryostat sections from a cell pellet were fixed in a buffered isotonic solution of 4% (v/v) formaldehyde for 5 min, and washed in running tap water for 5 min. Then, sections were incubated in 85% (v/v) propyleneglycol for 2 min (the solution was changed twice) and in Oil Red O [0.5% (v/v) in propyleneglycol] for 30 min. After rinsing in 85% (v/v) propyleneglycol for 1 min (the solution was changed twice), slides were washed twice in distilled water. Finally, sections were counterstained in hematoxylin for 30 s and mounted in AQUATEX® (Merck, Darmstadt, Germany).

Statistical analyses

The paired Student's *t*-test (two-tailed) was used to test the significance of the differences between group means. Statistical significance was defined as $P < 0.05$.

Acknowledgements

This work was funded by the Inova Foundation for Medical Research/The American Portuguese Biomedical Research Fund (APBRF, USA). The authors would like to thank L. Mayer and K. Uchida for providing antibodies, A. do Vale, F. Pisarra and M.T. Silva for help and comments on TEM, and M. Santos and R. Hultcrantz for critical reading of the manuscript. We also thank M. de Sousa for mentoring this work. M.C. and C.F.P. were supported by a fellowship from Inova/APBRF. E.M.C. was partially supported by EU grant (QLG1-CT-1999–00665).

References

1 Feder JN, Gnirke A, Thomas W, Tsuchihashi Z, Ruddy DA & Basava A (2003) The discovery of the new haemochromatosis gene 1996. *J Hepatol* **38**, 704–709.
2 Wilson IA & Bjorkman PJ (1998) Unusual MHC-like molecules: CD1, Fc receptor, the hemochromatosis gene product, and viral homologs. *Curr Opin Immunol* **10**, 67–73.
3 Zhou XY, Tomatsu S, Fleming RE, Parkkila S, Waheed A, Jiang J, Fei Y, Brunt EM, Ruddy DA, Prass CE *et al.* (1998) HFE gene knockout produces mouse model of hereditary hemochromatosis. *Proc Natl Acad Sci USA* **95**, 2492–2497.
4 Levy JE, Montross LK, Cohen DE, Fleming MD & Andrews NC (1999) The C282Y mutation causing hereditary hemochromatosis does not produce a null allele. *Blood* **94**, 9–11.
5 Santos M, Schilham MW, Rademakers LH, Marx JJ, de Sousa M & Clevers H (1996) Defective iron homeostasis in beta 2-microglobulin knockout mice recapitulates hereditary hemochromatosis in man. *J Exp Med* **184**, 1975–1985.

6 Olynyk JK, Cullen DJ, Aquilia S, Rossi E, Summerville L & Powell LW (1999) A population-based study of the clinical expression of the hemochromatosis gene. *New Engl J Med* **341**, 718–724.
7 Levy JE, Montross LK & Andrews NC (2000) Genes that modify the hemochromatosis phenotype in mice. *J Clin Invest* **105**, 1209–1216.
8 Beutler E (2003) The HFE Cys282Tyr mutation as a necessary but not sufficient cause of clinical hereditary hemochromatosis. *Blood* **101**, 3347–3350.
9 Porto G, Vicente C, Teixeira MA, Martins O, Cabeda JM, Lacerda R, Goncalves C, Fraga J, Macedo G, Silva BM *et al.* (1997) Relative impact of HLA phenotype and CD4-CD8 ratios on the clinical expression of hemochromatosis. *Hepatology* **25**, 397–402.
10 Arosa FA, Oliveira L, Porto G, da Silva BM, Kruijer W, Veltman J & de Sousa M (1997) Anomalies of the CD8+ T cell pool in haemochromatosis: HLA-A3-linked expansions of CD8+CD28- T cells. *Clin Exp Immunol* **107**, 548–554.
11 Cardoso EM, Hagen K, de Sousa M & Hultcrantz R (2001) Hepatic damage in C282Y homozygotes relates to low numbers of CD8+ cells in the liver lobuli. *Eur J Clin Invest* **31**, 45–53.
12 Cardoso EM, Macedo MG, Rohrlich P, Ribeiro E, Silva MT, Lemonnier FA & de Sousa M (2002) Increased hepatic iron in mice lacking classical MHC class I molecules. *Blood* **100**, 4239–4241.
13 Stal P, Broome U, Scheynius A, Befrits R & Hultcrantz R (1995) Kupffer cell iron overload induces intercellular adhesion molecule-1 expression on hepatocytes in genetic hemochromatosis. *Hepatology* **21**, 1308–1316.
14 Barisani D, Meneveri R, Ginelli E, Cassani C & Conte D (2000) Iron overload and gene expression in HepG2 cells: analysis by differential display. *FEBS Lett* **469**, 208–212.
15 George DK, Goldwurm S, MacDonald GA, Cowley LL, Walker NI, Ward PJ, Jazwinska EC & Powell LW (1998) Increased hepatic iron concentration in nonalcoholic steatohepatitis is associated with increased fibrosis. *Gastroenterology* **114**, 311–318.
16 Bonkovsky HL, Jawaid Q, Tortorelli K, LeClair P, Cobb J, Lambrecht RW & Banner BF (1999) Non-alcoholic steatohepatitis and iron: increased prevalence of mutations of the HFE gene in non-alcoholic steatohepatitis. *J Hepatol* **31**, 421–429.
17 Mendler MH, Turlin B, Moirand R, Jouanolle AM, Sapey T, Guyader D, Le Gall JY, Brissot P, David V & Deugnier Y (1999) Insulin resistance-associated hepatic iron overload. *Gastroenterology* **117**, 1155–1163.
18 Naidenko OV, Maher JK, Ernst WA, Sakai T, Modlin L & Kronenberg M (1999) Binding and antigen presentation of ceramide-containing glycolipids by soluble mouse and human CD1d molecules. *J Exp Med* **190**, 1069–1080.
19 Porcelli SA & Modlin RL (1999) The CD1 system: antigen-presenting molecules for T cell recognition of lipids and glycolipids. *Annu Rev Immunol* **17**, 297–329.
20 Blumberg RS, Terhorst C, Bleicher P, McDermott FV, Allan CH, Landau SB, Trier JS & Balk SP (1991) Expression of a nonpolymorphic MHC class I-like molecule, CD1D, by human intestinal epithelial cells. *J Immunol* **147**, 2518–2524.
21 Canchis PW, Bhan AK, Landau SB, Yang L, Balk SP & Blumberg RS (1993) Tissue distribution of the non-polymorphic major histocompatibility complex class I-like molecule, CD1d. *Immunology* **80**, 561–565.
22 Briken V, Moody DB & Porcelli SA (2000) Diversification of CD1 proteins: Sampling the lipid content of different cellular compartments. *Sem Immunol* **12**, 517–525.
23 Sugita M, Cernadas M & Brenner MB (2004) New insights into pathways for CD1-mediated antigen presentation. *Curr Opin Immunol* **16**, 90–95.
24 Grootveld M, Bell JD, Halliwell B, Aruoma OI, Bomford A & Sadler PJ (1999) Non-transferrin-bound iron in plasma or serum from patients with idiopathic hemochromatosis: characterization by high performance liquid chromatography and nuclear magnetic resonance spectroscopy. *J Biol Chem* **264**, 4417–4422.
25 Uchida K (1999) Current status of acrolein as a lipid peroxidation product. *Trends Cardiovasc Med* **9**, 109–113.
26 Bilsland CA & Milstein C (1991) The identification of the beta 2-microglobulin binding antigen encoded by the human CD1D gene. *Eur J Immunol* **21**, 71–78.
27 Shinkai K & Locksley RM (2000) CD1, tuberculosis, and the evolution of major histocompatibility complex molecules. *J Exp Med* **191**, 907–914.
28 Campbell NA, Kim HS, Blumberg RS & Mayer L (1999) The nonclassical class I molecule CD1d associates with the novel CD8 ligand gp180 on intestinal epithelial cells. *J Biol Chem* **274**, 26259–26265.
29 Han O, Fleet JC & Wood RJ (1999) Reciprocal regulation of HFE and NRamp2 gene expression by iron in human intestinal cells. *J Nutr* **129**, 98–104.
30 Tallkvist J, Bowlus CL & Lonnerdal B (2000) Functional and molecular responses of human intestinal Caco-2 cells to iron treatment. *Am J Clin Nutr* **72**, 770–775.
31 Hubert N, Lescoat G, Sciot R, Moirand R, Jego P, Leroyer P & Brissot P (1993) Regulation of ferritin and transferrin receptor expression by iron in human hepatocyte cultures. *J Hepatol* **18**, 301–312.
32 Hagen K, Zhu C, Melefors O & Hultcrantz R (1999) Susceptibility of cultured rat hepatocytes to oxidative stress by peroxides and iron. The extracellular matrix affects the toxicity of tert-butyl hydroperoxide. *Int J Biochem Cell Biol* **31**, 499–508.
33 Houglum K, Ramm GA, Crawford DH, Witztum JL, Powell LW & Chojkier M (1997) Excess iron induces hepatic oxidative stress and transforming growth factor

beta1 in genetic hemochromatosis. *Hepatology* **26**, 605–610.
34 Staubli A & Boelsterli UA (1998) The labile iron pool in hepatocytes: prooxidant-induced increase in free iron precedes oxidative cell injury. *Am J Physiol* **274**, G1031–G1037.
35 Kaplán P, Doval M, Majerova Z, Lehotsky J & Racay P (2000) Iron-induced lipid peroxidation and protein modification in endoplasmic reticulum membranes. Protection by stobadine. *Int J Biochem Cell Biol* **32**, 539–547.
36 Arezzini B, Lunghi B, Lungarella G & Gardi C (2003) Iron overload enhances the development of experimental liver cirrhosis in mice. *Int J Biochem Cell Biol* **35**, 486–495.
37 Britton RS, Ramm GA, Olynyk J, Singh R, O'Neill R & Bacon BR (1994) Pathophysiology of iron toxicity. *Adv Exp Medical Biol* **356**, 239–253.
38 Rodionov DG, Nordeng TW, Pedersen K, Balk SP & Bakke, O (1999) A critical tyrosine residue in the cytoplasmic tail is important for CD1d internalization but not for its basolateral sorting in MDCK cells. *J Immunol* **162**, 1488–1495.
39 Jayawardena-Wolf J, Benlagha K, Chiu YH, Mehr R & Bendelac A (2001) CD1d endosomal trafficking is independently regulated by an intrinsic CD1d-encoded tyrosine motif and by the invariant chain. *Immunity* **15**, 897–908.
40 Kang SJ & Cresswell P (2002) Regulation of intracellular trafficking of human CD1d by association with MHC class II molecules. *EMBO J* **21**, 1650–1660.
41 Cleton MI, de Bruijn WC, van Blokland WT, Marx JJ, Roelofs JM & Rademakers LH (1988) Iron content and acid phosphatase activity in hepatic parenchymal lysosomes of patients with hemochromatosis before and after phlebotomy treatment. *Ultrastruct Pathol* **12**, 161–174.
42 Stal P, Glaumann H & Hultcrantz R (1990) Liver cell damage and lysosomal iron storage in patients with idiopathic hemochromatosis. A light and electron microscopic study. *J Hepatol* **11**, 172–180.
43 Myers BM, Prendergast FG, Holman R, Kuntz SM & LaRusso NF (1991) Alterations in the structure, physicochemical properties, and pH of hepatocyte lysosomes in experimental iron overload. *J Clin Invest* **88**, 1207–1215.
44 Roberts TJ, Sriram V, Spence PM, Gui M, Hayakawa K, Bacik I, Bennink JR, Yewdell JW & Brutkiewicz RR (2002) Recycling CD1d1 molecules present endogenous antigens processed in an endocytic compartment to NKT cells. *J Immunol* **168**, 5409–5414.
45 Dillon SR, Constantinescu A & Schlissel MS (2001) Annexin V binds to positively selected B cells. *J Immunol* **166**, 58–71.
46 Melián A, Geng Y-J, Sukhova GK, Libby P & Porcelli SA (1999) CD1 expression in human atherosclerosis. A potential mechanism for T cell activation by foam cells. *Am J Pathol* **155**, 775–786.
47 Bonish B, Jullien D, Dutronc Y, Huang BB, Modlin R, Spada FM, Porcelli SA & Nickoloff BJ (2000) Overexpression of CD1d by keratinocytes in psoriasis and CD1d-dependent IFN-gamma production by NK-T cells. *J Immunol* **165**, 4076–4085.
48 Page MJ, Poritz LS, Tilberg AF, Zhang WJ, Chorney MJ & Koltun WA (2000) CD1d-restricted cellular lysis by peripheral blood lymphocytes: relevance to the inflammatory bowel disease. *J Surg Res* **92**, 214–221.
49 Ulanova M, Torebring M, Porcelli SA, Bengtsson U, Magnunson J, Magnunson O, Lin XP, Hanson LA & Telemo E (2000) Expression of CD1d in the duodenum of patients with cow's milk hypersensitivity. *Scand J Immunol* **52**, 609–617.
50 Tsuneyama K, Yasoshima M, Harada K, Hiramatsu K, Gershwin ME & Nakanuma Y (1998) Increased CD1d expression on small bile duct epithelium and epithelioid granuloma in livers in primary biliary cirrhosis. *Hepatology* **28**, 620–623.
51 Arosa FA (2002) CD8 + CD28- T cells: Certainties and uncertainties of a prevalent human T cell subset. *Immunol Cell Biol* **80**, 1–13.
52 Durante-Mangoni E, Wang R, Shaulov A, He Q, Nasser I, Afdhal N, Koziel MJ & Exley MA (2004) Hepatic CD1d expression in hepatitis C virus infection and recognition by resident proinflammatory CD1d-reactive T cells. *J Immunol* **173**, 2159–2166.
53 Hirayama M, Kohgo Y, Kondo H, Shintani N, Fujikawa K, Sasaki K, Kato J & Niitsu Y (1993) Regulation of iron metabolism in HepG2 cells: a possible role for cytokines in the hepatic deposition of iron. *Hepatology* **18**, 874–880.
54 Fadok VA, Bratton DL, Rose DM, Pearson A, Ezekewitz RA & Henson PM (2000) A receptor for phosphatidylserine-specific clearance of apoptotic cells. *Nature* **405**, 85–90.
55 Huynh ML, Fadok VA & Henson PM (2002) Phosphatidylserine-dependent ingestion of apoptotic cells promotes TGF-beta1 secretion and the resolution of inflammation. *J Clin Invest* **109**, 41–50.
56 Van Lenten BJ, Prieve J, Navab M, Hama S, Lusis AJ & Fogelman AM (1995) Lipid-induced changes in intracellular iron homeostasis in vitro and in vivo. *J Clin Invest* **95**, 2104–2110.
57 Brunet S, Thibault L, Delvin E, Yotov W, Bendayan M & Levy E (1999) Dietary iron overload and induced lipid peroxidation are associated with impaired plasma lipid transport and hepatic sterol metabolism in rats. *Hepatology* **29**, 1809–1817.
58 Woolfson A & Milstein C (1994) Alternative splicing generates secretory isoforms of human CD1. *Proc Natl Acad Sci USA* **91**, 6683–6687.